R. & M. No. 3258

MINISTRY OF AVIATION

AERONAUTICAL RESEARCH COUNCIL
REPORTS AND MEMORANDA

Some Possible Effects of Transonic Speeds on Wing-Aileron Flutter

By E. G. Broadbent and E. Violet Hartley

LONDON: HER MAJESTY'S STATIONERY OFFICE
1962
PRICE 6*s.* 6*d.* NET

Some Possible Effects of Transonic Speeds on Wing-Aileron Flutter

By E. G. Broadbent and E. Violet Hartley

Communicated by the Deputy Controller Aircraft (Research and Development), Ministry of Aviation

*Reports and Memoranda No. 3258**

January, 1959

Summary. A typical wing-aileron combination is taken and ternary flutter calculations between wing bending, wing torsion and aileron rotation are described. The results are plotted as graphs of flutter speed against aileron frequency and the effects of changes in aerodynamic derivatives such as might occur at transonic speeds are investigated. The derivative changes are (1) reduction first in $(-h_{\dot{\beta}})$ and then in all $\dot{\beta}$ derivatives and (2) aft shift of wing aerodynamic centre and aileron aerodynamic centre, separately and together.

1. *Introduction.* It is well known that aerodynamic derivatives can change rapidly at transonic speeds, but the precise nature of these changes cannot be predicted. It is, however, known that for wing-aileron flutter the most important general trends are:

(1) a reduction of the damping derivatives associated with control-surface rotation, (the $\dot{\beta}$ derivatives);

(2) an aft shift in the centres of lift, first due to aileron deflection and then due to wing incidence.

These effects are often investigated qualitatively on supersonic aircraft, but it was felt that a survey in which a few parameters were varied systematically would help in understanding the problem. As this type of work is suitable for the flutter simulator, a typical problem was taken from the simulator records, this being thought more suitable than using a hypothetical wing-aileron combination. The problem relates to a swept-back wing with conventional wing-tip ailerons (Fig. 1). The parameters varied were:

(1) Circuit stiffness

(2) Mass-balance (zero and static only)

(3) $-h_{\dot{\beta}}$ (the direct aerodynamic damping on the aileron)

(4) all the $\dot{\beta}$ derivatives

(5) $-m_{\beta}/I_{\beta}$ (position of lift due to aileron)

(6) $-m_{\alpha}/I_{\alpha}$ (position of lift due to wing incidence).

Ternary calculations involving wing bending, wing torsion and aileron rotation were carried out, and curves of flutter speed against aileron frequency have been plotted, and are discussed in Section 3.

* Previously issued as R.A.E. Tech. Note No. Structures 258—A.R.C. 21,055.

It is a particular advantage of the flutter simulator that complete curves of this type can very quickly be plotted once the basic coefficients are known. In an analytical paper written some time ago and before the application of electronic computers and simulators to flutter work, Buxton and Minhinnick[1] derived expressions for the rate of change of critical flutter speed with flutter coefficients. As one of their examples, similar to that of the present Paper, they consider ternary control-surface flutter involving the degrees of freedom aircraft pitch, fuselage bending and elevator rotation. With control-surface flutter, however, the change in the overall size and shape of the stability boundaries is of much greater importance than the local variation of the critical flutter speed and for this reason the emphasis is placed on such boundary changes in the present Paper.

2. *Basic Data.* The problem is a typical flutter calculation with wing bending, wing torsion and aileron rotation. The aerodynamic derivatives were varied systematically to represent transonic effects. A swept-back wing was used. The details of geometry are:

Leading-edge sweep	49 deg
Hinge-line sweep	27 deg
Aerodynamic balance	Nil
Aspect ratio	2·85

The basic derivatives were calculated for zero Mach number, using the Minhinnick rules for quasi-static theory. The modes were calculated normal modes, primarily wing bending and wing torsion, with a frequency ratio of 0·25:1. The flutter coefficients used on the simulator for zero mass-balance are given in Table 1 below.

TABLE 1

	Mode 1	Mode 2	Mode 3
a	1110	95	138
b	84	17	271
c	42	78	625
d			
e	131		
a	+ 95	+ 612	138
b	− 6	+ 39	121
c	− 10	− 15	228
d			
e		+1110	
a	138	138	424
b	9	14	326
c	2	5	373
d			
e			Variable

Blanks in the Table indicate zero coefficients

Mode 1 is wing bending
Mode 2 is wing torsion
Mode 3 is aileron rotation

The coefficients are derived from the standard simulator flutter equation

$$[a\ddot{q} + bv\dot{q} + cv^2q + d\dot{q} + eq] = 0$$

where

$v = \frac{V}{V_0}$, and V_0 is a chosen arbitrary reference speed

q_r Generalised co-ordinate of mode r

$\dot{q} = \frac{dq}{d\tau}$ where τ is a non-dimensional time parameter

a Matrix of inertia coefficients

b Matrix of aerodynamic damping coefficients

c Matrix of aerodynamic stiffness coefficients

d Matrix of structural damping coefficients

e Matrix of structural stiffness coefficients.

As the wing bending and wing torsion modes are calculated normal modes, the cross inertias and cross stiffness coefficients (a_{12}, a_{21}, e_{12}, e_{21}) should be zero. However the mass distribution was altered after the calculation of the normal modes, but the original modal shapes were retained. As a result e_{12} and e_{21} are still zero, but a_{12} and a_{21} are finite. Structural damping was neglected: the inclusion of damping would tend to decrease the flutter regions, but for small amounts of damping the general shape would be maintained. The aileron circuit stiffness, e_{33}, was treated as a variable, and no separate circuit freedom, *e.g.*, to represent power controls, was included.

The two inertia cases considered were zero and static mass-balance, the inertia coefficients for static mass-balance being the elements of the following 'a' matrix which is consistent with Table 1.

TABLE 2

$$\begin{bmatrix} 1110 & 95 & 36 \\ 95 & 612 & 79 \\ 36 & 79 & 540 \end{bmatrix}$$

The mass-balance was distributed along the leading edge of the control, and as would be expected it had a more powerful effect in reducing a_{13} than a_{23}.

The nodal lines of the two modes are shown in Fig. 1. It will be noticed that the nodal line for the mode of wing torsion by no means follows the classical pattern of lying along the wing main spar, and in fact looks more like the nodal line of an overtone bending mode. On wings of lowish aspect ratio, however, torsion and overtone bending do tend to influence each other, and in the present case the amplitudes increase very rapidly towards the tip so that considerable torsion does occur over that part of the wing containing the aileron. Also shown on Fig. 1 is the locus of aerodynamic centres due to wing incidence at low speed; the reference value is taken to be that at the mid-aileron position where it lies at 20 per cent of the wing chord aft of the leading edge.

The height for which the coefficients were calculated was 10,000 ft. The basic (1, 3) and (2, 3) binaries for heights of sea level, 10,000 ft, 20,000 ft and 40,000 ft were previously investigated. An altitude of 10,000 ft was actually chosen because the (2, 3) binary gave flutter speeds at heights

greater than 10,000 ft, and it was thought that this condition in which the torsion branch was just absent with full values of the derivatives would provide an interesting example. In any case a height of about 10,000 ft might well represent the worst case in practice for torsion aileron flutter on this aircraft, because of the high dynamic pressures.

The basic ternary calculation gave a small region of flutter as shown in Fig. 2 where v is plotted against ω_3/ω_2, the aileron to wing torsion frequency ratio. The flutter is of (1, 3) binary type and is eliminated altogether by static balance. The wing flutter speed [(1, 2) binary] was outside the simulator range, a desk calculation giving $v = 3{\cdot}45$.

3. *Results of Calculations.* 3.1. *Variations to Simulate Transonic Effects.* The variations adopted fall into two classes, the reduction of aerodynamic damping on the one hand, and the aft shift of the aerodynamic centres on the other. The changes made are discussed below under these two headings. Two aerodynamic centres are important in the present work and both of these are on the wing and in each case their position is expressed as a fraction of the wing chord aft of the leading edge. The first is the aerodynamic centre due to wing incidence and the second is that due to applied aileron angle. They will be described in the present Paper as 'aerodynamic centre due to incidence' and 'aerodynamic centre due to aileron' respectively. The former refers to the point at which the incremental lift on the wing acts due to an increment of wing incidence and the latter refers to the point at which the incremental lift on the wing acts due to an increment of aileron angle. In both cases it is that component of the force which is in phase with the displacement that is referred to, *i.e.*, the relevant derivatives are the aerodynamic stiffness derivatives and exclude the aerodynamic damping derivatives.

(*a*) Loss in aerodynamic damping.

(1) Reduction in direct aileron damping alone ($-h_{\dot{\beta}}$).

(2) Reduction in all $\dot{\beta}$ derivatives ($-h_{\dot{\beta}}$), ($-m_{\dot{\beta}}$) and ($l_{\dot{\beta}}$).

In both cases the factor on the basic value was varied from $+1{\cdot}0$ to $-0{\cdot}6$ in stages of $0{\cdot}4$, for both zero and static balance.

(*b*) Shift in aerodynamic centres.

(1) Aft shift of aerodynamic centre due to aileron ($-m_\beta/l_\beta$).

With the aerodynamic centre due to incidence in its low speed position at 20 per cent chord at the mid-aileron section (Fig. 1) the aerodynamic centre due to aileron was shifted aft from 52 per cent local wing chord to $83{\cdot}2$ per cent chord in three equal stages, for zero and static balance.

(2) Aft shift of aerodynamic centre due to incidence ($-m_\alpha/l_\alpha$).

With the aerodynamic centre due to aileron in its low speed position at 52 per cent chord, the aerodynamic centre due to incidence was shifted aft from 20 per cent chord at aileron semi-span to 40 per cent chord, in four equal steps.

(3) Aft shift of aerodynamic centre due to incidence with an aft position of aerodynamic centre due to aileron.

The aerodynamic centre due to incidence was shifted aft from 20 per cent chord at the aileron semi-span to 25 per cent chord and 40 per cent chord for a further aft position of the aerodynamic centre due to aileron ($83{\cdot}2$ per cent) in the condition of static mass-balance only. This was done because in practice the aerodynamic centre due to aileron probably moves aft first.

3.2. *Presentation of Results.* The results are given in the form of graphs of v, which should be regarded simply as the flutter speed plotted to an arbitrary scale, against ω_3/ω_2 for different parameters. A coincidence between the aileron frequency (at zero air speed) and the frequency of the wing torsion mode, is indicated by a value of ω_3/ω_2 of 1·0, and a coincidence between the aileron frequency (at zero air speed) and the frequency of the wing bending mode is indicated by a value of ω_3/ω_2 of 0·255.

Many of the results showed two separate flutter regions. The low speed curve was primarily the (1, 3) binary and tended to be eliminated when $\omega_3 > \omega_1$. The curve at higher speed was mainly the (2, 3) binary and this tended to be eliminated when $\omega_3 > \omega_2$. The low speed curve was more responsive to mass-balance variations than was the higher speed curve, a result which is to be expected since the mass-balance is more effective against wing bending than wing torsion (*see* Tables 1 and 2).

3.3. *Discussion of Results.* 3.3.1. *Reduction of* $(-h_{\dot\beta})$ *alone.* The basic value of $(-h_{\dot\beta})$ is multiplied by a factor K_1, which is varied from unity downwards, and the results are indicated in tabular form.

TABLE 3

Mass-balance condition	K_1	Speed range	Remarks	Dominant wing mode	Fig. No.
Zero	1 to 0·2	0·040 to 0·750	Little effect other than extending the nose of the curve from ω_3/ω_2 of 0·24 to 0·3.	Bending	2
	0·6	1·200 to 2·050	Higher speed curve introduced at $K_1 = 0·6$ which rapidly extends and	Torsion	
	0·2	0·250 to 2·200	when $K_1 = 0·2$ the flutter speed falls as ω_3/ω_2 approaches 1·0.	Torsion	
	−0·2 to −0·6	0 to 2·200	Complete instability.	—	
Static	1	Stable	—	—	3
	0·6 to 0·2	0·060 to 0·550	Lower speed curve is introduced and the flutter speed falls as ω_3 approaches coincidence with ω_1.	Bending	
		0·550 to 1·950	Upper speed branch is introduced and the flutter speed falls rapidly as ω_3 approaches coincidence with ω_2.	Torsion	
			Both branches are much narrower than at zero mass-balance.		
	−0·2 to −0·6	0 to > 2·200	Complete instability.		

3.3.2. *Reduction in all* $\dot\beta$ *derivatives.* The basic values of $(-h_{\dot\beta})$, $(-m_{\dot\beta})$ and $(l_{\dot\beta})$ are all multiplied by a factor K_2 which is varied from unity downwards, and the results are indicated in tabular form.

TABLE 4

Mass-balance condition	K_2	Speed range	Remarks	Dominant wing mode	Fig. No.
Zero	1 to 0·2	0·150 to 0·650	The nose of the basic curve is again extended but the fall in flutter speed at coincidence of frequencies is not so great as when $(-h_{\dot{\beta}})$ alone is varied.	Bending	4
	0·6 to 0·2	1·250 to 2·100	The higher speed branch is again introduced at $K_2 = 0·6$, but is much less extensive than when $(-h_{\dot{\beta}})$ alone is varied.	Torsion	—
	−0·2 to −0·6		Complete instability.	—	—
Static	1		Stable		5
	0·6 to 0·2	0·100 to 0·530	The lower speed branch is again introduced, and is again much narrower than for zero mass-balance. The nose of the curve extends to $\omega_3 = \omega_2$ and the flutter speed falls considerably at this point.	Bending	
	0·2	1·050 to 1·950	The higher speed branch is not introduced until K_2 falls to 0·2. It extends further than at zero mass-balance.	Torsion	
	−0·2 to −0·6	0 to > 2·200	There is again complete instability when K_2 becomes negative.	—	

The decrease in the flutter regions when all the $\dot{\beta}$ derivatives, $(-h_{\dot{\beta}})$, $(-m_{\dot{\beta}})$ and $(l_{\dot{\beta}})$, are varied together when compared with the flutter regions obtained when $(-h_{\dot{\beta}})$ is varied alone, is evidently due to a stabilizing effect arising from the reduction of $(-m_{\dot{\beta}})$ and $(l_{\dot{\beta}})$.

The effect of reduction in the $\dot{\beta}$ derivatives is similar to that caused by an increase in altitude. The latter is equivalent to a reduction in all the damping derivatives for the same equivalent air speed, and this is the reason that the torsion aileron branch first appears and then grows considerably in extent as the altitude is increased.

3.3.3. *Aft shift of aerodynamic centre due to aileron.* The basic value of $(-m_{\beta})$ is multiplied by a factor K_3 which is varied from 1 to 1·6, and the results are indicated in TABLE 5 overleaf.

3.3.4. *Aft shift of aerodynamic centre due to incidence.* The basic value of $(-m_{\alpha})$ is multiplied by a factor K_4 which is varied from 1 to 2, and the results are indicated in TABLE 6 overleaf.

3.3.5. *Aft shift of aerodynamic centre due to incidence with an aft position of aerodynamic centre due to aileron given by* $K_3 = 1·6$. The basic value of $(-m_{\alpha})$ is multiplied by the factor K_4 which is varied from 1 to 2 and the results indicated in tabular form TABLE 7 overleaf.

TABLE 5

Mass-balance condition	K_3	Speed range	Remarks	Dominant wing mode	Fig. No.
Zero	1 to 1·6	0·120 to 0·775	The curve of the basic case ($K_3 = 1$) is extended as K_3 increases. The nose of the curve approaches $\omega_3/\omega_1 = 1·1$ for $K_3 = 1·6$.	Bending	6
	1·2 to 1·6	0·800 to > 2·2	The upper speed curve is introduced when $K_3 = 1·2$ and extends rapidly, the critical flutter speed falling as ω_3/ω_2 approaches 1·0.	Torsion	
Static	1	Stable			7
	1·2 to 1·6	0·750 to > 2·2	The lower branch is not present over the range covered, but the upper branch is introduced when $K_3 = 1·2$. The flutter speed falls as ω_3/ω_2 approaches 1·0. The flutter area is less than for zero mass-balance.	Torsion	

TABLE 6

Mass-balance condition	K_4	Speed range	Remarks	Dominant wing mode	Fig. No.
Zero	1·0	0·130 to 0·700	Only this lower branch is present, and there is very little change in the flutter region.	Bending	8
Static	1·0 to 2·0	Stable	Complete stability occurs over the whole range of K_4.		

TABLE 7

Mass-Balance condition	K_4	Speed range	Remarks	Dominant wing mode	Fig. No.
Static	1·0 to 2·0	0·730 to > 2·2	Only the upper branch is present and there is little variation from the value of $K_4 = 1$.	Torsion	9

4. *Conclusions.* In the present Paper arbitrary variations in the aerodynamic derivatives such as might occur at transonic speeds have been made, and the effects on a typical wing aileron problem have been investigated. For the most part the flutter is of the coupled type, either bending-aileron or torsion-aileron, but when the direct aileron aerodynamic damping is reduced to zero, flutter in one degree of freedom occurs throughout the speed range. In all cases the coupled flutter is prevented by a sufficiently high circuit stiffness, but the results presented give no indication of the effect of circuit stiffness on the flutter in one degree of freedom. In practice there will be some effect because increase of circuit stiffness leads to a higher frequency parameter which helps to suppress the loss of damping. A criterion sometimes used in this connection is that $\Omega c_\beta > 100$, where Ω is the aileron natural frequency in cycles per second and c_β is the aileron chord in feet[2]. In principle therefore, a high circuit stiffness can be used to prevent all forms of aileron flutter.

If mass-balance is used as a means of flutter prevention the results obtained indicate that it alone provides no safeguard against the loss in aerodynamic damping and it also becomes less effective against torsion-aileron flutter as the aerodynamic centre due to aileron moves aft. Furthermore if static balance is combined with moderate circuit stiffness, torsion-aileron flutter may occur at quite low speeds. These results therefore confirm the authors' view that mass-balance should not be used as a flutter preventive on supersonic aircraft. It should however, be added that the results apply to a particular planform and further work is necessary before making general conclusions. It is known, for example, that for some aircraft, calculations have shown no sharp dividing line between stability and instability as $(-h_{\dot{\beta}})$ passes through zero[3].

LIST OF SYMBOLS

The derivative notation used is as follows. Other notation is defined in the text as it occurs.

$$dL = \rho V^2 c\,dy\{(-\nu^2 l_{\ddot{z}} + i\nu l_{\dot{z}} + l_z)\frac{z}{c} + (-\nu^2 l_{\ddot{\alpha}} + i\nu l_{\dot{\alpha}} + l_\alpha)\alpha + (-\nu^2 l_{\ddot{\beta}} + i\nu l_{\dot{\beta}} + l_\beta)\beta$$

$$dM = \rho V^2 c^2\,dy\{(-\nu^2 m_{\ddot{z}} + i\nu m_{\dot{z}} + m_z)\frac{z}{c} + (-\nu^2 m_{\ddot{\alpha}} + i\nu m_{\dot{\alpha}} + m_\alpha)\alpha + (-\nu^2 m_{\ddot{\beta}} + i\nu m_{\dot{\beta}} + m_\beta)\beta$$

$$dH = \rho V^2 c^2\,dy\{(-\nu^2 h_{\ddot{z}} + i\nu h_{\dot{z}} + h_z)\frac{z}{c} + (-\nu^2 h_{\ddot{\alpha}} + i\nu h_{\dot{\alpha}} + h_\alpha)\alpha + (-\nu^2 h_{\ddot{\beta}} + i\nu h_{\dot{\beta}} + h_\beta)\beta$$

dL	Lift force on a strip dy
dM	Nose-up pitching moment about the leading edge on a strip dy
dH	Nose-up hinge moment on a strip dy
z	Down displacement at the leading edge of the strip
α	Nose-up wing rotation of the strip
β	Nose-up control surface angle of the strip relative to the wing
ρ	Air density
V	Forward speed
c	Wing chord at the current spanwise position y
ν	Frequency parameter $\omega c/V$ where ω is the frequency
$l_{\ddot{z}} \ldots . h_{\ddot{\beta}}$	Aerodynamic inertia derivatives
$l_{\dot{z}} \ldots . h_{\dot{\beta}}$	Aerodynamic damping derivatives
$l_z \ldots . h_\beta$	Aerodynamic stiffness derivatives
	ω_r is the natural frequency of mode r taken alone
	All the displacements z, α and β are relative to the undisturbed position.

REFERENCES

No.	*Author*	*Title, etc.*
1	G. H. L. Buxton and I. T. Minhinnick	Expressions for the rates of change of critical flutter speeds and frequencies with inertial, aerodynamic and elastic coefficients. A.R.C. R. & M. 2444. September, 1945.
2	E. G. Broadbent	Aeroelastic problems in connection with high speed flight. *J.R.Ae.Soc.* July, 1956.
3	E. G. Broadbent	Flutter prediction in practice. Advisory Group for Aeronautical Research and Development. Report 44. April, 1956.

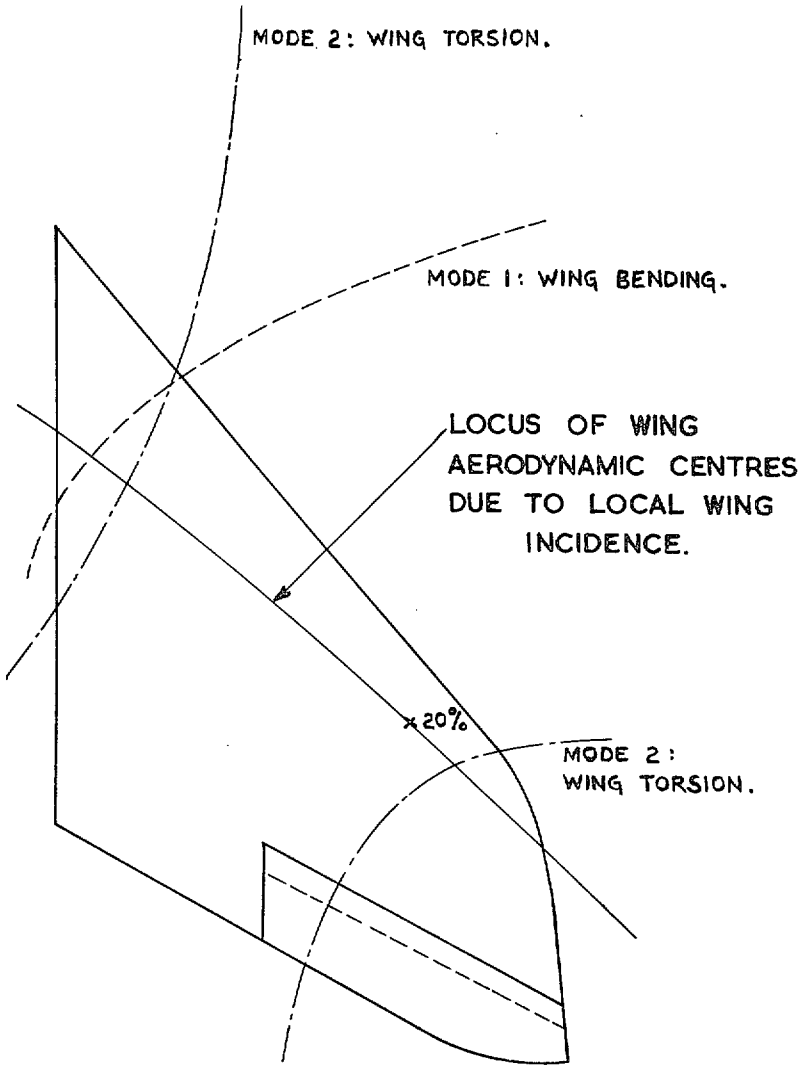

FIG. 1. Planform of wing considered.

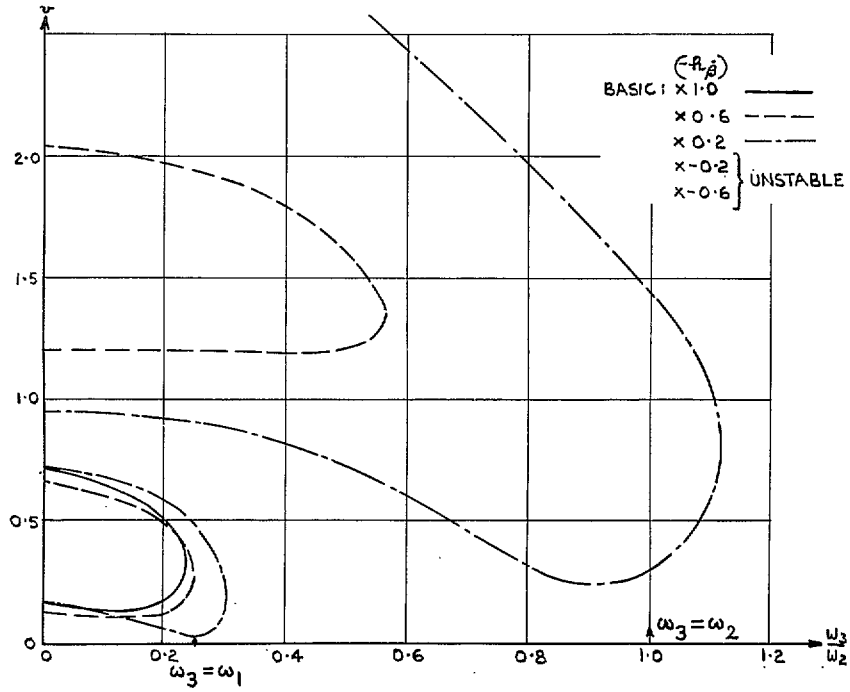

FIG. 2. Reduction in direct aileron damping alone. Zero mass-balance.

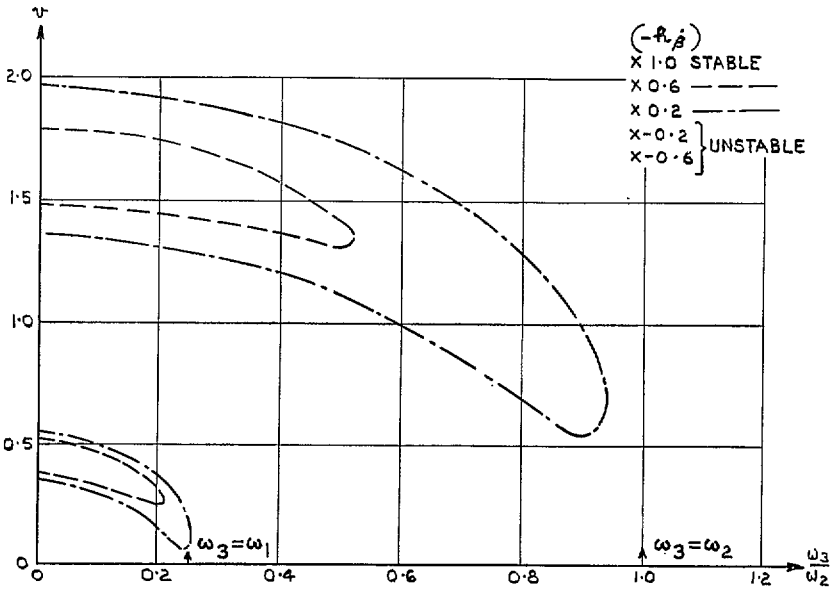

FIG. 3. Reduction in direct aileron damping alone. Static mass-balance.

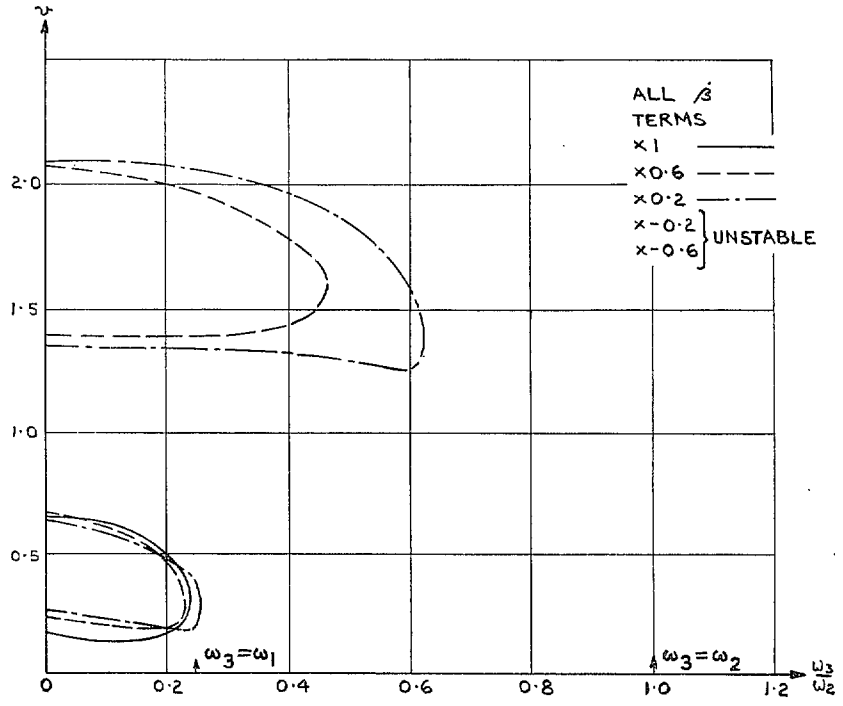

FIG. 4. Reduction in all $\dot{\beta}$ derivatives. Zero mass-balance.

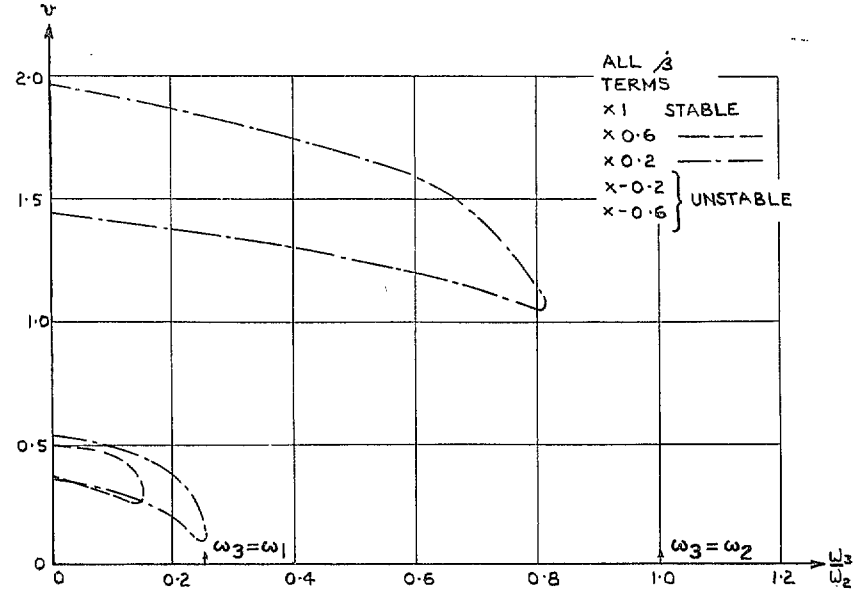

FIG. 5. Reduction in all $\dot{\beta}$ derivatives. Static mass-balance.

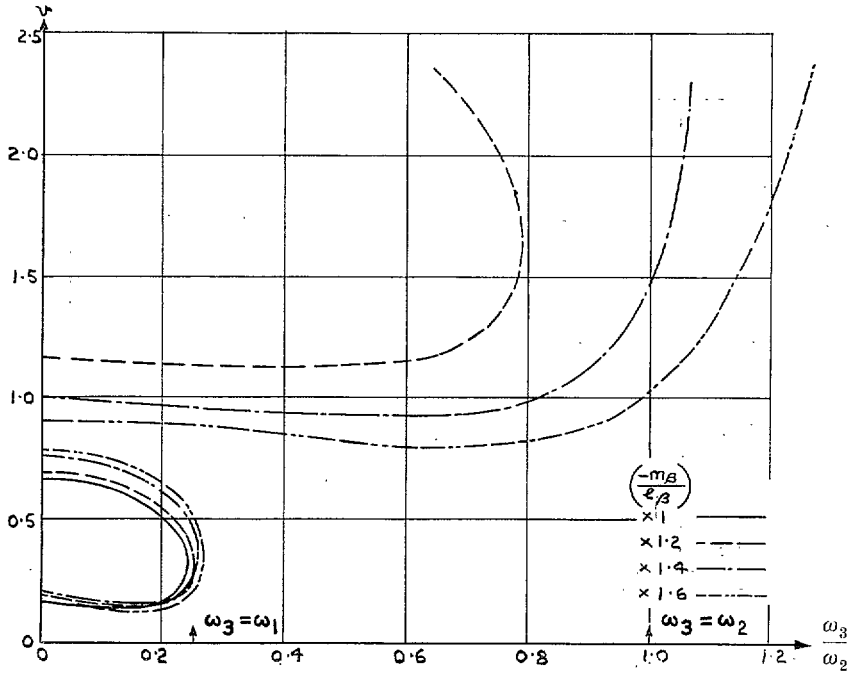

FIG. 6. Aft shift of aerodynamic centre due to aileron. Zero mass-balance.

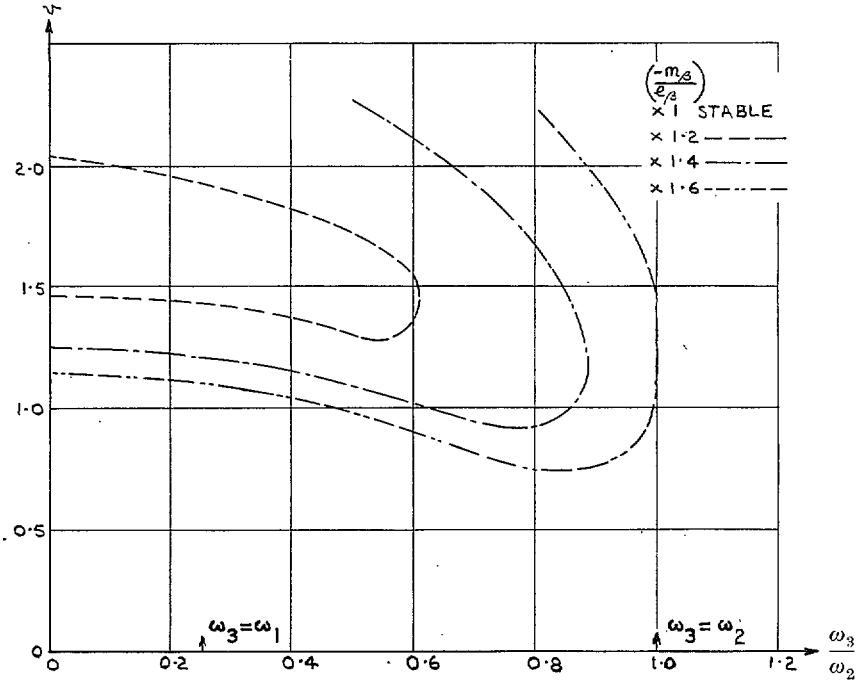

FIG. 7. Aft shift of aerodynamic centre due to aileron. Static mass-balance.

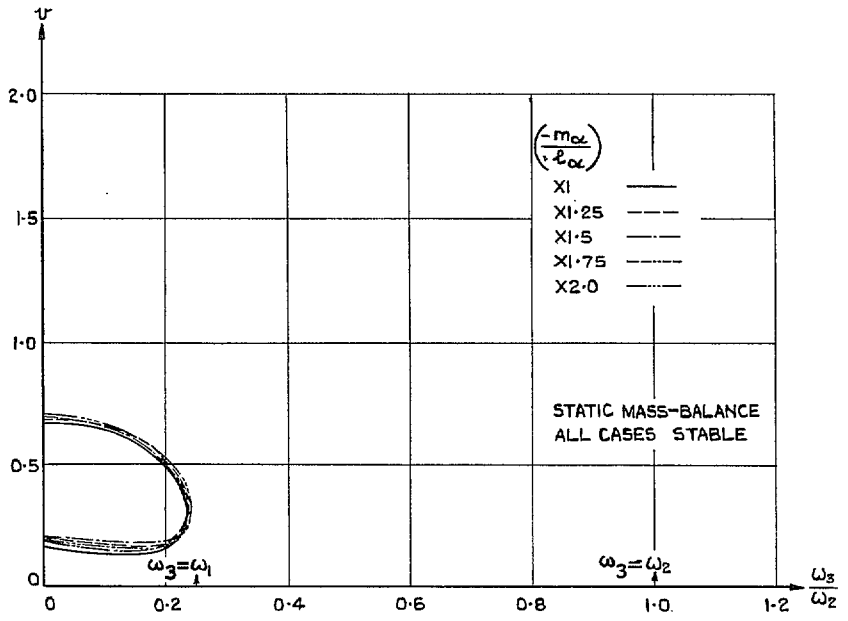

FIG. 8. Aft shift of aerodynamic centre due to incidence. Zero mass-balance.

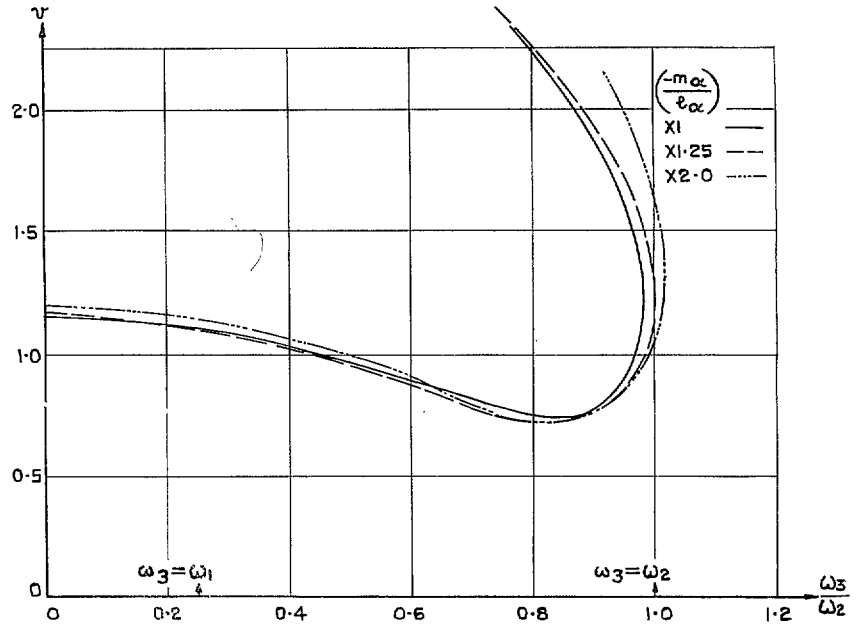

FIG. 9. Aft shift of aerodynamic centre due to incidence with aerodynamic centre due to aileron at 83·2 per cent chord. Static mass-balance.

(83823) Wt. 67/1876 K.5 3/62 Hw.

Publications of the Aeronautical Research Council

ANNUAL TECHNICAL REPORTS OF THE AERONAUTICAL RESEARCH COUNCIL (BOUND VOLUMES)

1941 Aero and Hydrodynamics, Aerofoils, Airscrews, Engines, Flutter, Stability and Control, Structures. 63*s.* (post 2*s.* 3*d.*)

1942 Vol. I. Aero and Hydrodynamics, Aerofoils, Airscrews, Engines. 75*s.* (post 2*s.* 3*d.*)
Vol. II. Noise, Parachutes, Stability and Control, Structures, Vibration, Wind Tunnels. 47*s.* 6*d.* (post 1*s.* 9*d.*)

1943 Vol. I. Aerodynamics, Aerofoils, Airscrews. 80*s.* (post 2*s.*)
Vol. II. Engines, Flutter, Materials, Parachutes, Performance, Stability and Control, Structures. 90*s.* (post 2*s.* 3*d.*)

1944 Vol. I. Aero and Hydrodynamics, Aerofoils, Aircraft, Airscrews, Controls. 84*s.* (post 2*s.* 6*d.*)
Vol. II. Flutter and Vibration, Materials, Miscellaneous, Navigation, Parachutes, Performance, Plates and Panels, Stability, Structures, Test Equipment, Wind Tunnels. 84*s.* (post 2*s.* 6*d.*)

1945 Vol. I. Aero and Hydrodynamics, Aerofoils. 130*s.* (post 3*s.*)
Vol. II. Aircraft, Airscrews, Controls. 130*s.* (post 3*s.*)
Vol. III. Flutter and Vibration, Instruments, Miscellaneous, Parachutes, Plates and Panels, Propulsion. 130*s.* (post 2*s.* 9*d.*)
Vol. IV. Stability, Structures, Wind Tunnels, Wind Tunnel Technique. 130*s.* (post 2*s.* 9*d.*)

1946 Vol. I. Accidents, Aerodynamics, Aerofoils and Hydrofoils. 168*s.* (post 3*s.* 3*d.*)
Vol. II. Airscrews, Cabin Cooling, Chemical Hazards, Controls, Flames, Flutter, Helicopters, Instruments and Instrumentation, Interference, Jets, Miscellaneous, Parachutes. 168*s.* (post 2*s.* 9*d.*)
Vol. III. Performance, Propulsion, Seaplanes, Stability, Structures, Wind Tunnels. 168*s.* (post 3*s.*)

1947 Vol. I. Aerodynamics, Aerofoils, Aircraft. 168*s.* (post 3*s.* 3*d.*)
Vol. II. Airscrews and Rotors, Controls, Flutter, Materials, Miscellaneous, Parachutes, Propulsion, Seaplanes, Stability, Structures, Take-off and Landing. 168*s.* (post 3*s.* 3*d.*)

Special Volumes

Vol. I. Aero and Hydrodynamics, Aerofoils, Controls, Flutter, Kites, Parachutes, Performance, Propulsion, Stability. 126*s.* (post 2*s.* 6*d.*)
Vol. II. Aero and Hydrodynamics, Aerofoils, Airscrews, Controls, Flutter, Materials, Miscellaneous, Parachutes, Propulsion, Stability, Structures. 147*s.* (post 2*s.* 6*d.*)
Vol. III. Aero and Hydrodynamics, Aerofoils, Airscrews, Controls, Flutter, Kites, Miscellaneous, Parachutes, Propulsion, Seaplanes, Stability, Structures, Test Equipment. 189*s.* (post 3*s.* 3*d.*)

Reviews of the Aeronautical Research Council

1939–48 3*s.* (post 5*d.*) 1949–54 5*s.* (post 5*d.*)

Index to all Reports and Memoranda published in the Annual Technical Reports

1909–1947 R. & M. 2600 6*s.* (post 2*d.*)

Indexes to the Reports and Memoranda of the Aeronautical Research Council

Between Nos. 2351–2449	R. & M. No. 2450 2*s.* (post 2*d.*)
Between Nos. 2451–2549	R. & M. No. 2550 2*s.* 6*d.* (post 2*d.*)
Between Nos. 2551–2649	R. & M. No. 2650 2*s.* 6*d.* (post 2*d.*)
Between Nos. 2651–2749	R. & M. No. 2750 2*s.* 6*d.* (post 2*d.*)
Between Nos. 2751–2849	R. & M. No. 2850 2*s.* 6*d.* (post 2*d.*)
Between Nos. 2851–2949	R. & M. No. 2950 3*s.* (post 2*d.*)
Between Nos. 2951–3049	R. & M. No. 3050 3*s.* 6*d.* (post 2*d.*)

HER MAJESTY'S STATIONERY OFFICE

from the addresses overleaf

Printed and published by
HER MAJESTY'S STATIONERY OFFICE

To be purchased from
York House, Kingsway, London W.C.2
423 Oxford Street, London W.1
13A Castle Street, Edinburgh 2
109 St. Mary Street, Cardiff
39 King Street, Manchester 2
50 Fairfax Street, Bristol 1
35 Smallbrook, Ringway, Birmingham 5
80 Chichester Street, Belfast 1
or through any bookseller

Printed in England

R. & M. No. 3258

S.O. Code No. 23-3258